A novel approach to design structural natural fiber composites from sustainable CO_2-derived polyhydroxyurethane thermosets with outstanding properties and circular features

Guillem Seychal[1,2], Pierre Nickmilder[3], Vincent Lemaur[4], Connie Ocando[1], Bruno Grignard[5,6], Philippe Leclère[3], Christophe Detrembleur[5], Roberto Lazzaroni[4], Haritz Sardon[2], Nora Aramburu[*2], and Jean-Marie Raquez[†1]

[1]*Laboratory of Polymeric and Composite Materials, Center of Innovation and Research in Materials and Polymers (CIRMAP), University of Mons, Place du Parc 23, Mons, 7000, Belgium*
[2]*POLYMAT and Department of Advanced Polymers and Materials: Physics, Chemistry, and Technology, Faculty of Chemistry, University of the Basque Country UPV/EHU, Paseo Manuel de Lardizabal 3, Donostia-San Sebastián, 20018, Spain*
[3]*Laboratory for Physics of Nanomaterials and Energy (LPNE), Research Institute for Materials Science and Engineering, University of Mons (UMONS), 20 Place du Parc, B-7000 Mons, Belgium*
[4]*Laboratory for Chemistry of Novel Materials, Research Institute for Materials Science and Engineering, University of Mons, Place du Parc 23, Mons, 7000, Belgium*
[5]*Department of Chemistry, Center for Education and Research on Macromolecules (CERM), University of Liège, Sart-Tilman, B6A, Liège, 4000, Belgium*
[6]*FRITCO$_2$T Platform, University of Liege, Sart-Tilman B6a, 4000 Liege, Belgium*

Supplementary Informations

Contents

[*]nora.aramburu@ehu.eus
[†]jean-marie.raquez@umons.ac.be

List of Figures

I Complementary materials and methods

I.1 Synthesis of TMPTC

In a typical experiment, TMPTE (1 L, 1.157 kg) was transferred into a 2 L high-pressure reactor. Then, 35.29 g of TBAI (2.5 mol% vs TMPTE) was added before closing the cell. The cell was then equilibrated at 110 °C for 24 h, keeping a constant 90 bar CO_2 pressure and a 200 rpm stirring rate. After the reaction, the stirring was stopped, the cell was slowly depressurized at 110 °C, and the viscous product was collected and analyzed by ^{1}H-NMR in $CDCl_3$ (Supp. Fig. 1). TMPTC was produced with a yield of >98% (collected crude product >1.4 kg). Before use, the product was degassed under vacuum treatment at 60 °C for 16 h. Monomer properties are summarized in Supp.Tab.1.

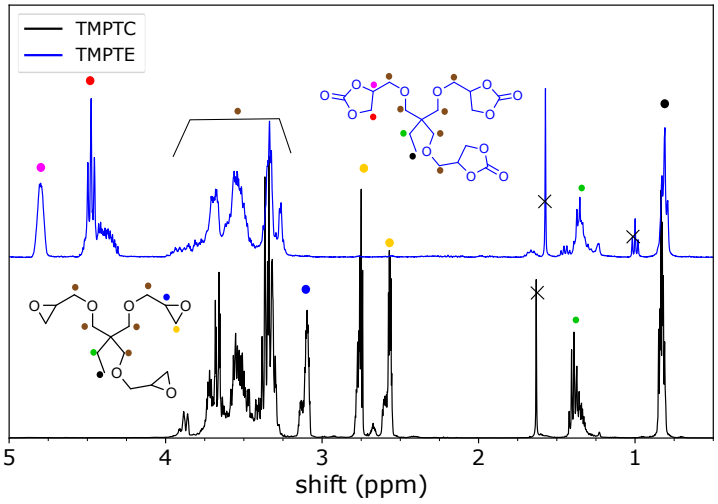

Supp. Fig. 1: ^{1}H-NMR in $CDCl_3$ of the epoxy precursor (TMPTE) and the resulting carbonate (TMPTC)

I.2 Material properties

Name	Ref	EEW (g/eq)	CEW (g/eq)	$\eta_{25°C}$ (Pa.s)
TrimethylolPropane Triglycidyl Ether	TMPTE	140	-	0.15
TrimethylolPropane TriCarbonate	TMPTC	-	175	148

Supp. Tab. 1: Monomer properties

Name	Areal Weight g/m^2	ρ g/cm^3	E$_L$ GPa	E$_T$ GPa	$\boldsymbol{\sigma}_{break}$ MPa	$\boldsymbol{\varepsilon}_{break}$ %	Reference
UD Flax fibers	110	1.39	59	8	975	2.1	[1, 2, 3]
UD Carbon fibers	100	1.82	240	17	4900	2.0	Supplier

Supp. Tab. 2: Properties of the reinforcements for Rule-of-Mixture

I.3 Characterization

I.3.1 Fourier transform infrared (FTIR)

Fourier Transform Infrared spectra in attenuated total reflectance mode were performed on a Bruker FTIR Tensor 27 spectrometer over a range of $4000 - 600$ cm^{-1} with a 4 cm^{-1} resolution.

I.3.2 Rheological measurements

The curing rheological behavior of unreacted matrices was measured on an Anton Paar Modular Compact Rheometer MCR302 in isothermal mode at 80 °C. About 1.5 g of product was used between two 25 mm diameter parallel aluminum plates, with a 1 mm separation. Measurements were performed with a 2% strain applied at 1 Hz.

I.3.3 Thermogravimetric analysis (TGA)

Thermal degradation of the materials (about 10mg) was performed on a TGAQ500 from TA Instruments between 25 and 800 °C at a heating rate of 20 °C/min under a 60 mL.min^{-1} N_2 flow.

I.3.4 Dynamic mechanical analysis (DMA)

Tensile DMA of the thermosets was conducted on a TA Instruments DMA Q800. 20x8x0.8 mm^3 rectangular samples were employed with a 10 mm gauge length. The DMA analysis was executed from -50 to 180 °C following a 3 °C/min. The 0.1% strain tension was applied at a 1 Hz frequency. The DMA results were used to identify the crosslinking density ($\nu_{E'}$) of the thermosets using the rubber elasticity theory as described in eq (1).

$$\nu_{E'} = \frac{E'_{T_{\alpha+50}}}{3RT_{\alpha+50}} \tag{1}$$

with $T_{\alpha+50}$ the temperature of the rubbery plateau set 50 K after the α transition taken at the maximum of the $\tan\delta$ curve, $E'_{T_{\alpha+50}}$ the storage modulus in Pa at the specified temperature and R the perfect gas constant (8.314 J mol^{-1} K^{-1}).

I.3.5 Monotonic mechanical properties of the thermosets and composites

The neat thermosets' mechanical behavior was investigated through monotonic tensile testing following ASTM D638 standard. A ZwickRoell Z2.5 equipment with a 2.5 kN cell force was used. Tests were performed at a 1 mm/min displacement rate up to failure. For each material, five type V dog-bone shape samples were tested up to failure. Young's modulus was calculated by linear regression between 0.1% and 1.0% strain.

The three-point monotonic bending properties of the composites as ascribed in ASTM D790, were investigated in both parallel and perpendicular to fibers' orientation load orientation. Five rectangular samples were tested with a 50.8x12.7x1.2 mm^3 geometry at 1 mm/min. A 0.1 MPa preload was used to ensure perfect contact. The bending modulus was evaluated between 0.1 and 0.5% bending strain by linear regression.

I.3.6 Vertical UL94 burning test

According to ASTM D3801-2010, samples of dimensions of 130 mm × 14 mm x 6 plies (as manufactured) were used to assess the fire behavior of the composites. Ignition for 10 s in air atmosphere was done using a Bunsen burner.

I.3.7 Scanning electron microscopy (SEM)

SEM images were taken out on a Hitachi's STEM FEG SU8020 instrument with 5.0 nm resolution in general mode up to 2.0 nm at 5 kV. Voltage ranged from 0.1 to 30 kV, and the magnification varied from 20 to 800k. A platinum-palladium coating of 9 nm was sprayed on samples.

I.3.8 Atomic force microscopy (AFM)

A Dimension Icon AFM with RTESPA 300 cantilevers (Bruker Corp.) was used to obtain the AFM Peak Force Tapping (PFT) measurements. The cantilevers possess a spring constant around 40 Nm^{-1} and a tip radius of 8 nm. The deflection sensitivity was determined with the help of a sapphire sample. The areas scanned were between 1.5 and 50 μm^2. The generated data were analyzed with the help of the Nanoscope Analysis software. Samples were prepared without embedding and cut with a diamond knife at -80 °C.

I.3.9 Density measurement

Density measurements have been conducted using Archimede's principle. Small square samples (for composites) of 10x10 mm^2 were laser cut. They were first weighed in air and then weighed in ethanol. Density was then calculated using (2) Three samples have been evaluated for each configuration to average results.

$$\rho = \frac{M_{air}}{M_{air} - M_{ethanol}}(\rho_{air} - \rho_{ethanol}) + \rho_{ethanol} \tag{2}$$

with M_{air} and $M_{ethanol}$ being the weight of the sample in the air and in the ethanol respectively. Fluid densities were taken as $\rho_{ethanol} = 0.79$ g/cm^3 and $\rho_{air} = 0.0012$ g/cm^3.

I.3.10 Gel Content

The gel content (GC) of the formulations was determined in THF. Three samples of about 20 mg were weighted (m_0) and soaked in solvent. Samples were then collected and dried at 80 °C under vacuum for 24 h and weighted (m_2). The GC was calculated using eq.(3)

$$GC = \frac{m_2}{m_0} * 100 \tag{3}$$

II Optimization of the PHU matrix

Prior to composite manufacturing, the PHU formulation was optimized by adding different types and amounts of catalysts. Considering composite manufacturing processes, catalysts can enhance the curing time but can also drastically decrease the processability [4]. For each catalyst, 1 mol%,5 mol%, and 10 mol% were considered with respect to CC functions. Isothermal rheological tests during the curing were performed at 80°C. Results are summarized in Supp. Tab. 3. The evolution of viscosity, storage, and loss modulus over time can be found in Supp. Fig. 4 and Supp. Fig. 3. Overall results highlight the importance of the catalyst and the catalytic load over the curing of these mixtures. Only 1 mol % of DMAP or DBU was found to already positively affect the curing. To reach the gel point, 49 and 51 min at 80°C were necessary compared to the original 83 min, representing a decrease of about 40%. Interestingly, the pot life was not significantly affected at these levels with 20 and 19 min respectively compared to 23 min for the non-catalyzed system. Surprisingly, a higher amount of DMAP did not lead to an important change in the curing behavior with no observable change in the pot life and a gel time dropping down to 41 min with 10 mol% of DMAP. Therefore, a threshold effect could be considered in the case of DMAP, and higher amounts are not required. The catalytic effect was reported to be greatly influenced by hydrogen bonding during polymerization [5, 6]. Consequently, this behavior could be related to the increase of the H-bonding that can decrease the catalytic effect of DMAP not being strong enough to act when the viscosity becomes too high [7]. Contrary to DMAP, DBU amount was shown to significantly modify the curing behavior. If 1% of DBU shows the same trends as DMAP, the reaction occurs much faster at room temperature with 5% of load. The faster start of the reaction was highlighted by the increase in the initial viscosity, reaching 83 Pa.s with 10% of DBU. Along the initial viscosity, the pot life was decreased up to 4 min and the gel time was reduced to 20 min. The improved catalytic effect of DBU on the catalysis of PHU polymerization was reported in literature [6]. However, PHUs being investigated for adhesives, the requirements on catalyst effect differ from composite manufacturing [4]. Indeed, DBU catalytic effect appears to be detrimental to the processing window. Such behavior reflects the importance of the catalyst type and amount on the processability.

The amount of catalyst could also play an effect on the mechanical properties. In this work, it was assumed that the catalyst could act as a plasticizer and therefore decrease the glass transition or the glassy modulus [8]. For these reasons, the effect of catalyst was studied by DMA for 10% of DMAP or DBU respectively. The extracted values are reported in Supp. Tab. 3 and the graph can be found in Supp. Fig. 3a. Infrared spectroscopy was also performed and depicted in Supp. Fig. 3b. With 10% of catalyst load, the FTIR reveals the appearance of urea signals at 1650 cm^{-1}. These urea linkages are due to side reactions promoted by the catalyst as previously reported in literature [9, 5]. The presence of a catalyst also led to a decrease of about 20% of the storage modulus with 10% load. However, the alpha transition (T_α) was seemingly not influenced nor the crosslinking density by the presence of a catalyst. With 10% of DMAP, the evolution of $\tan\delta$ exhibits two peaks that could be related to the presence of the urea linkage and potential phase separation [10]. Considering the effect of the catalyst on the processability and the final properties, 1% of DMAP was kept for the rest of the present study in the TMC formulation.

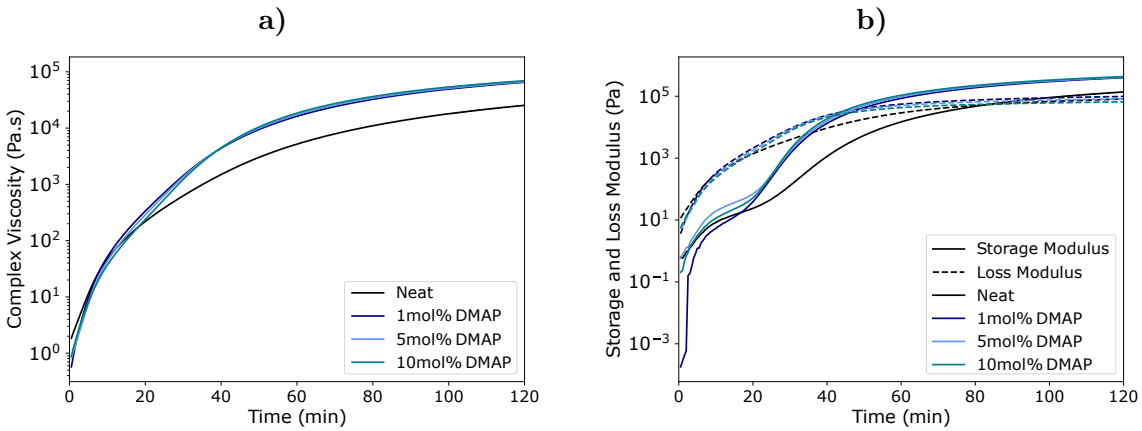

Supp. Fig. 2: DMAP catalyst effect on a) Viscosity evolution of the TMX-MX formulations, and b) Modulus evolution during curing rheological behavior at 80°C

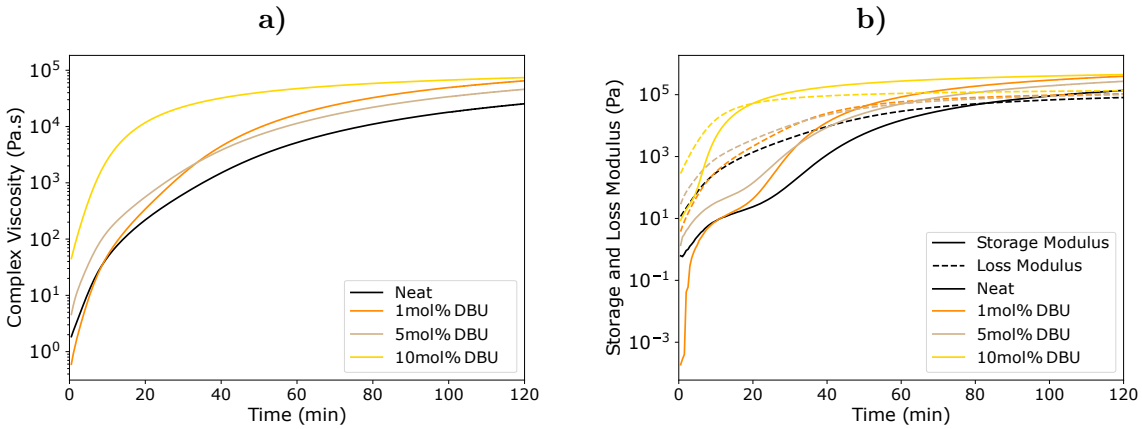

Supp. Fig. 3: DBU catalyst effect on a) Viscosity evolution of the TMX-MX formulations, and b) Modulus evolution during curing rheological behavior at 80°C

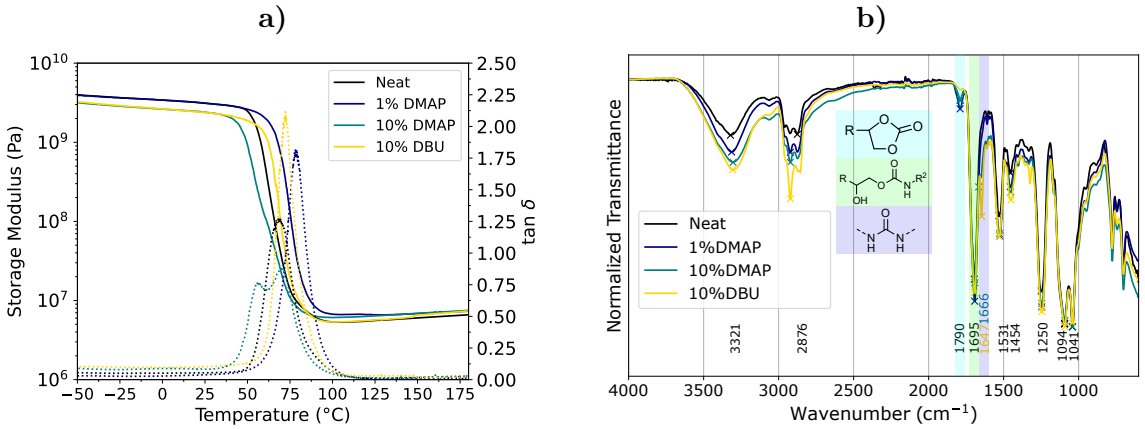

Supp. Fig. 4: a) Effect of catalyst on thermo-mechanical properties, and b) FTIR of the cured TMC-MX thermosets with catalyst load

			Neat	1% DMAP	5% DMAP	10% DMAP	1% DBU	5% DBU	10% DBU
Isothermal rheology	η_{init}	Pa.s	2.8	1.3	1.4	1.6	1.3	8.9	82.5
	Pot Life	min	23	19	20	21	19	15	4
	Gel Time	min	83	49	45	41	51	60	20
DMA	T_α	$°C$	69	78	-	70	-	-	72
	$E'_{25°C}$	MPa	3121	3129	-	2405	-	-	2374
	$E'_{rubbery}$	MPa	5.5	6.58	-	6.3	-	-	5.6
	ν'_e	mol/m^3	559	657	-	642	-	-	569

Supp. Tab. 3: Effect of catalyst on curing and thermo-mechanical properties of PHUs

III Comparison between PHU (TMC) and epoxy EP (TME) thermosets - additional results

III.1 Rheological properties

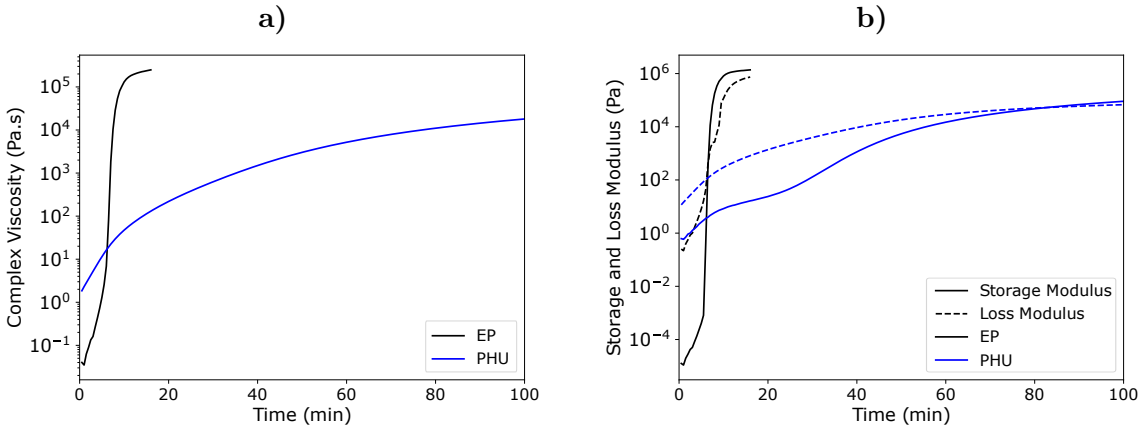

Supp. Fig. 5: Isothermal curing (80°C) of epoxy and PHU in rheometer.a) Viscosity evolution, and b) Modulus evolution over time

III.2 Thermal stability

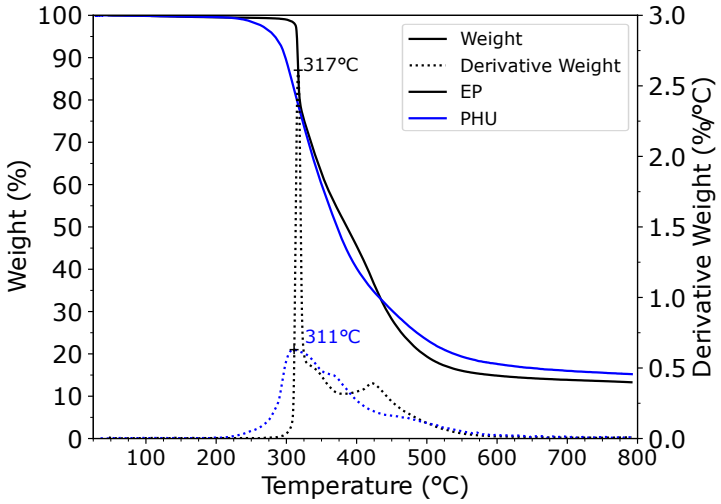

Supp. Fig. 6: TGA under N_2 flow of epoxy and PHU matrix

III.3 Mechanical properties - Tensile tests

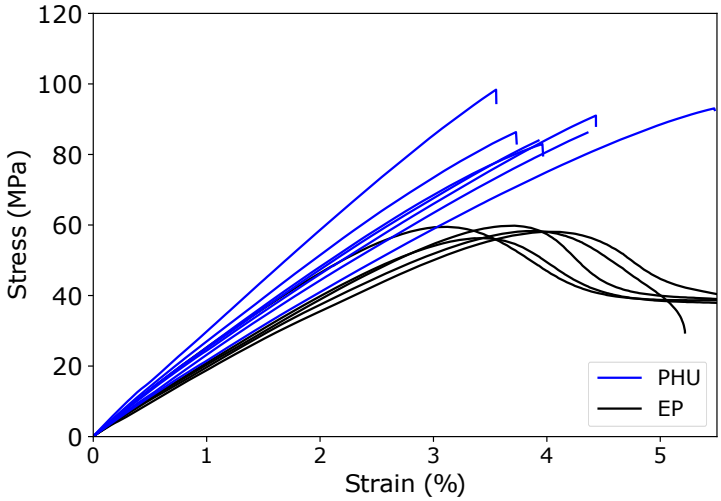

Supp. Fig. 7: Tensile tests of PHU and epoxy matrix

IV Comparison between PHU-flax (F-TMC) and epoxy-flax (TME) structural composites - additional results

IV.1 PHU-carbon and epoxy-carbon composites-microstructure

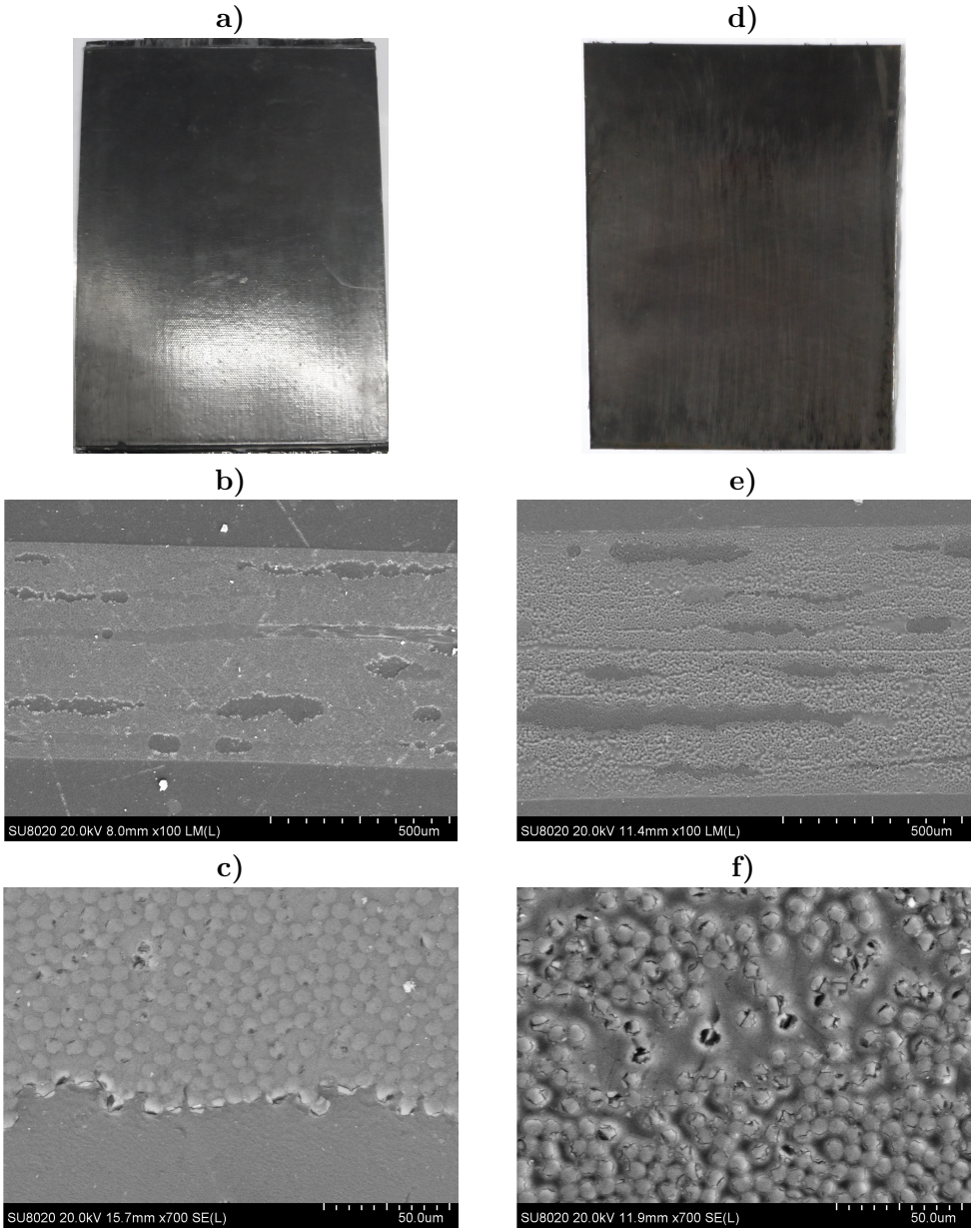

Supp. Fig. 8: Pictures of the manufactured laminates, SEM cross-sections images with x80 magnifications and x700 magnifications (top to bottom) for a-c) C-EP, and d-f) C-PHU

IV.2 PHU-carbon and epoxy-carbon composites-mechanical properties

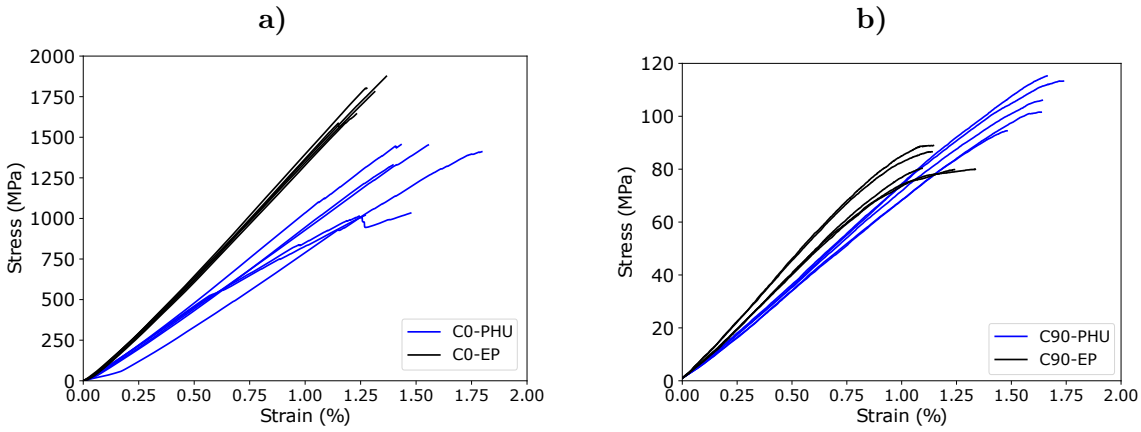

Supp. Fig. 9: Three-point bending of the carbon fiber reinforced polymers for the laminates a) $[0]_6$ b)$[90]_6$

IV.3 Thermal stability of composites

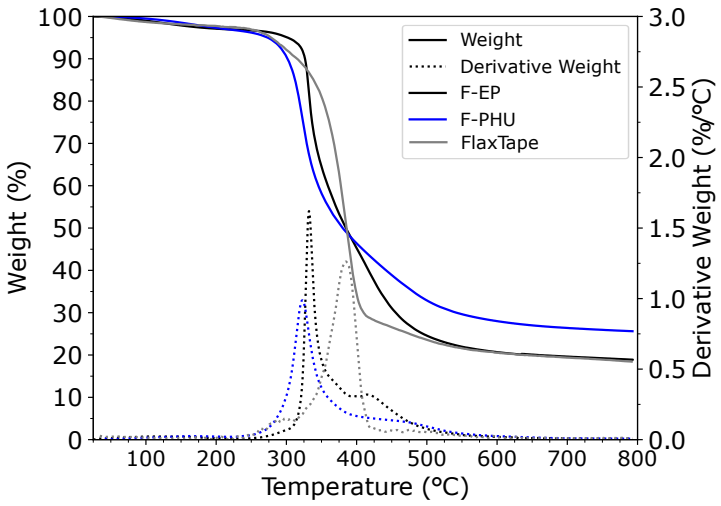

Supp. Fig. 10: TGA under N_2 flow of the flax laminates

V Welding of composites - Complementary results

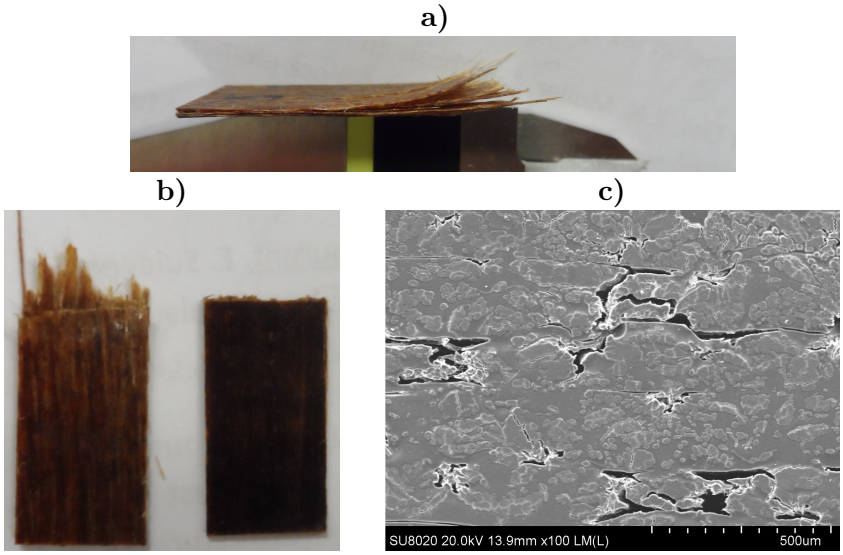

Supp. Fig. 11: a) Broken "welded" F-EP laminates with delamination b) comparison of the broken welded samples epoxy matrix (left) and PHU matrix (right), and c) SEM image of the F-EP laminate

References

[1] Le Gall M, Davies P, Martin N, Baley C. Recommended flax fibre density values for composite property predictions. Industrial Crops and Products. 2018 Apr;114:52-8.

[2] Baley C, Perrot Y, Busnel F, Guezenoc H, Davies P. Transverse tensile behaviour of unidirectional plies reinforced with flax fibres. Materials Letters. 2006:4.

[3] Baley C, Bourmaud A. Average tensile properties of French elementary flax fibers. Materials Letters. 2014 May;122:159-61.

[4] Advani SG, Hsiao KT. 1 - Introduction to composites and manufacturing processes. In: Advani SG, Hsiao KT, editors. Manufacturing Techniques for Polymer Matrix Composites (PMCs). Woodhead Publishing Series in Composites Science and Engineering. Woodhead Publishing; 2012. p. 1-12.

[5] Blain M, Cornille A, Boutevin B, Auvergne R, Benazet D, Andrioletti B, et al. Hydrogen bonds prevent obtaining high molar mass PHUs. Journal of Applied Polymer Science. 2017 Dec;134(45):44958.

[6] Maisonneuve L, Lamarzelle O, Rix E, Grau E, Cramail H. Isocyanate-Free Routes to Polyurethanes and Poly(hydroxy Urethane)s. Chemical Reviews. 2015 Nov;115(22):12407-39.

[7] Bobbink FD, van Muyden AP, Dyson PJ. *En route* to CO $_2$ -containing renewable materials: catalytic synthesis of polycarbonates and non-isocyanate polyhydroxyurethanes derived from cyclic carbonates. Chemical Communications. 2019;55(10):1360-73.

[8] Park SJ, Seo MK, Lee JR, Lee DR. Studies on epoxy resins cured by cationic latent thermal catalysts: The effect of the catalysts on the thermal, rheological, and mechanical properties. Journal of Polymer Science Part A: Polymer Chemistry. 2001;39(1):187-95.

[9] Cornille A, Auvergne R, Figovsky O, Boutevin B, Caillol S. A perspective approach to sustainable routes for non-isocyanate polyurethanes. European Polymer Journal. 2017 Feb;87:535-52.

[10] Beniah G, Liu K, Heath WH, Miller MD, Scheidt KA, Torkelson JM. Novel thermoplastic polyhydroxyurethane elastomers as effective damping materials over broad temperature ranges. European Polymer Journal. 2016 Nov;84:770-83.